Comparison and Fitting of Analytical Expressions to Existing Data for the Critical-Band Concept

Florian Völk[1,2)]

[1)] Bio-Inspired Information Processing, Institute of Medical Engineering, Technische Universität München, Boltzmannstraße 11, 85748 Garching, Germany. voelk@tum.de

[2)] WindAcoustics UG (haftungsbeschränkt), Mühlbachstraße 1, 86949 Windach, Germany.

Summary

The existing analytical expressions describing the frequency dependencies of critical bandwidth and equivalent-rectangular bandwidth were derived from the results of different sets of listening experiments. As the corresponding band-rate scales are constructed by integrating the reciprocal bandwidth function over frequency, also the band-rate functions are based on the respectively selected experiments. The critical-bandwidth formula converges to 100 Hz at frequencies below about 500 Hz and the critical-band-rate function is not invertible in closed form, which complicates the application of the critical-band concept in modeling. In order to overcome these restrictions, the data used earlier to construct and validate the bandwidth functions were re-evaluated separately for the critical-band and the equivalent-rectangular-band concepts, and also combined. It is shown that the shape of a critical-bandwidth-frequency formula derived from a cochlear frequency-position function that results in an invertible critical-band-rate formula can be fitted to both data sets. Depending on frequency, the formulae predict about 1.53 to 1.55 times larger critical than equivalent-rectangular bandwidths. Low-frequency critical bandwidths, which are overestimated compared to the data by the earlier formula, are represented more accurately and at the same time suited better to avoid modeling artifacts. The determined functions are compared against each other and against the previously proposed bandwidth and band-rate formulae. The results indicate that a common function shape with a simple parameter variation is suited to account for the data used earlier to validate two different sets of formulae.

PACS no. 43.66.-x, 43.66.Ba, 43.66.Cb, 43.71.An

1. Introduction

The concept of critical bands introduced by Zwicker and colleagues [1], based on studies of Fletcher and coworkers [2], describes frequency bands of frequency-dependent spectral width with no fixed position on the frequency scale, as they appear in various psychoacoustic experiments ([3], pp. 150–158). Among those are studies on modulation detection [4], loudness summation [5], absolute thresholds [6], and masking patterns of narrow-band noises [7]. All these experiments show a change of results if the spectral width of one of the stimuli involved is increased beyond the critical bandwidth $\Delta f_{\mathrm{G}}(f)$. Therefore, the critical bands appear to correspond to a perceptual effect common to all these experiments, and consequently play an important role in modeling and explaining the associate perceptual mechanisms.

The original critical-band concept, as described in the previous paragraph, formalizes bandwidths as they appear in the results of different listening experiments. While a relationship to perceptual mechanisms is possible, no assumption about the underlying processes is contained in the concept. The peripheral hearing is a highly non-linear system with frequency-dependent and level-dependent transmission characteristics [3]. Therefore, the critical-band concept does not assume the existence or rely on what is often referred to as auditory filters; it may much rather be regarded as the average representation of a spectral selectivity effect observed similarly in different listening experiments at various levels [1, 3, 5].

Zwicker and colleagues defined the critical bandwidth at low frequencies symmetric on the linear frequency scale around the respective center frequency f (table 6.1, p. 160 of [3]). This symmetry will cause critical-band-wide analysis channels to select negative frequencies if the critical bandwidth exceeds double the corresponding center frequency, that is if $\Delta f_{\mathrm{G}}(f) > 2f$. Bandpass filtering with a filter extended beyond 0 Hz has no physical analogy and introduces undesired artifacts, which is also true for auditory-adapted Fourier-transform algorithms [8, 9, 10, 11]. The selection of negative frequencies oc-

Received 27 March 2015,
accepted 12 October 2015.

curs if $\Delta f_{\mathrm{G}}(f) > 2f$, even if ideal filtering is assumed, and can hardly be justified by psychoacoustic experiments. However, as Zwicker's critical bandwidths are constant at 100 Hz for center frequencies below some 500 Hz, selection of negative frequencies will occur with critical-band-wide filters centered at frequencies below 50 Hz.

Based on the critical bands, a critical-band-rate function $z(f)$ has been derived [12], relating frequency to critical-band rate so that all critical bands are equally wide on the critical-band-rate scale. Different formulae to calculate critical-band rate, its inverse $f(z)$, and critical bandwidth were proposed [13, 14, 15]. Only the latest provide an invertible critical-band-rate function reasonably valid for the complete audible frequency range, which is crucial for defining equally-distributed frequencies on the critical-band-rate scale. This is for example required if a predefined number of bandpass filters is to be distributed equally spaced on an auditory-adapted frequency scale. Völk [15] also proposed an extension of the original critical-bandwidth formula that ensures $\Delta f(f) \leqslant 2f$ and thereby avoids the above-mentioned artifacts due to selection of negative frequencies, resulting in a more universally applicable formula.

A framework similar to the critical bands, but actually assuming so-called auditory filters of specific shape was proposed by Moore and Glasberg [16, 17], based on the equivalent-rectangular bandwidths $\Delta f_{\mathrm{E}}(f)$ introduced by Patterson [18]. The corresponding formulae relating frequency to bandwidth and band rate differ from the critical-band functions in magnitude and shape. The equivalent-rectangular bands are smaller than the critical bands in general and especially at low center frequencies. For that reason, the selection of negative frequencies is rather unproblematic for equivalent-rectangular-band-wide filters.

The critical-band concept is frequently applied in different areas, for example in auditory-adapted Fourier transforms [8, 11], speech coding [9], signal and system analysis [10, 11, 19], instrumental loudness prediction [20, 21, 22], and signal processing for auditory prostheses such as hearing aids and cochlear implants [23, 24]. However, different arguments have been put forward, favoring one set of bandwidth and band-rate formulae over the other [25, 26, 27, 28, 29].

Rather than looking at the differences between the critical-band and equivalent-rectangular-band concepts, it is the aim of this paper to focus on their similarities and common features. This is especially interesting from an applied point of view, where the shape of the bandwidth function is often more important than its absolute magnitude, as scaling factors are used in most models, selecting a constant fraction of critical or equivalent-rectangular bandwidth [8, 9, 30]. In order to compare both concepts, previously published results from listening experiments used earlier to support both concepts were fitted separately and as a whole to the function shape proposed by Greenwood [31] based on a physiological point of view on cochlear frequency selectivity. The determined functions were compared against each other and against the previously proposed bandwidth and band-rate formulae. The results indicate that a common shape of the functions is rather plausible based on the data included in this study. The resulting function's low-frequency behavior is suited to reduce the above-mentioned selection of negative frequencies.

It is clear that such a view on the data is not appropriate or intended to explain the differences between the data sets or the underlying perceptual and decision mechanisms discussed elsewhere [25, 27, 28, 29]. Much rather, the analysis is meant to pave the way for a unified and most universally applicable critical-bandwidth formula, especially with regard to applications, in pointing out the global commonalities of the data. Such a formula will be of help in cases where a detailed explanation of underlying mechanisms is less necessary than an average relation between stimuli and subject reports. However, the analysis also shows that a common function shape with a simple parameter variation is suited to account for the data used earlier to validate two different sets of formulae.

The paper is structured as follows: After a brief review of the data and previously proposed formulae for the critical-band and equivalent-rectangular-band concepts, the fitting procedure is motivated and introduced. Then, the resulting fitting parameters are tabulated and compared. As a result, critical-bandwidth-function shape and parameters are proposed and shown to be, based on the data included, the best compromise available at this time. Concluding, the corresponding critical-band-rate function and its inverse are constructed and the formulae are given in closed form.

2. Critical bandwidth

According to Fastl and Zwicker [3], the level-independent critical bandwidths given by table 6.1 (p. 160) were determined by psychoacoustic measurements at various levels and frequencies with different experimental methods on more than 50 subjects ([3], p. 158). While the actual studies or data included remain unclear, the references given by Fastl and Zwicker combined with a literature review provide several studies that most likely served as a basis for the averaging process leading to the tabulated data, or later as validation data. An overview of these publications and the levels respectively loudness levels studied is given in table I. A common conclusion of all the studies is that the resulting bandwidths did not depend notably on the presentation level.

The critical bandwidth estimates of the studies listed in table I are shown as gray symbols in figure 1. Each cross represents an inter-individual median at a specific center frequency.

The critical bandwidths $\Delta f_{\mathrm{G}}[n]$ were tabulated initially by Zwicker [1] and (slightly modified) [12], as sample points $f_{\mathrm{c}}[n]$ with $n = 1, \ldots, 24$, indicated according to [12] by the filled black squares in figure 1. The tabulated values were reprinted by Zwicker and Terhardt [13] with a modification: the lowest critical bandwidth $\Delta f_{\mathrm{G}}[1] = 80$ Hz was changed to 100 Hz (diamond in figure 1; cf. also [3], p. 160).

Table I. Studies the critical-bandwidth estimates discussed in the present paper were taken from, with the respectively examined levels or loudness levels (average values) and numbers of participants N.

ID	Study	Data	(Loudness) Levels	N
1	Zwicker 1952 [4]	Abbildung 12	30, 40, 50, 60, 70, 80 phon	4
2	Zwicker 1954 [7]	Abbildung 7	40, 50, 60, 80 dB/tone	2
3	Gäßler 1954 [6]	Abbildung 7	10, 30, 50 dB/Hz	2
4	Zwicker 1955 [5]	Section 5 a)	20, 30, 40, 50, 60, 70, 80 dB	1
5	Bauch 1956 [32]	Abbildung 4	30, 45, 70 dB	2
6	Greenwood 1961 [31]	Table I	50, 55, 65, 75 dB	5
7 a	Schorer 1986a [26]	Figure 1 (open)	65 phon/tone	4
7 b	Schorer 1986a [26]	Figure 1 (filled)	65 phon/tone	4
8 a	Schorer 1986b [33]	Figure 5	80 dB	8
8 b	Schorer 1986b [33]	Figure 5	50 dB	8
8 c	Schorer 1986b [33]	Figure 5	20 dB SL	8

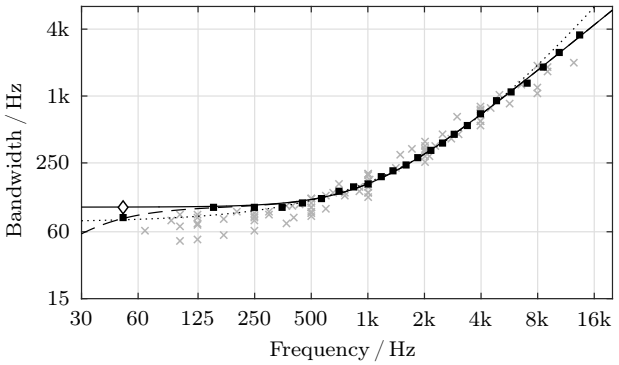

Figure 1. Inter-individual medians of the studies listed in table I (gray crosses). Filled black squares: values tabulated by Zwicker 1961 [12]; unfilled diamond: update according to Zwicker and Terhardt 1980 [13]. Black contours: Critical bandwidth $\Delta f_{\mathrm{G}}\,(f)$ according to Zwicker and Terhardt ([13], solid; equation 1 of the present paper), Traunmüller ([14], dotted), and Völk ([15], dashed; equation 4 of the present paper).

This modification appears to be done in order to achieve simple and continuous dependencies; especially to keep the critical bandwidth constant at 100 Hz for frequencies below about 500 Hz that is for $n = 1, \ldots, 5$. As an explanation, [3] state (p. 158):

> *Although the lowest critical bandwidth in the audible frequency region may be very close to 80* Hz*, it is attractive to add the inaudible range from 0* Hz *to 20* Hz *to that critical band, and to assume that the lowest critical band ranges from 0* Hz *to 100* Hz*.*

Based on the updated table, Zwicker and Terhardt ([13], indicated by the subscript Z) proposed the critical-bandwidth function

$$\frac{\Delta f_{\mathrm{G_Z}}\,(f)}{\mathrm{Hz}} = 25 + 75\left[1 + 1.4\left(\frac{f}{\mathrm{kHz}}\right)^2\right]^{0.69}, \qquad (1)$$

fitting the tabulated data of [13] with an accuracy of $\pm 10\%$, while deviating by 25% from the original value at $n = 1$ (solid black contour in figure 1; cf. [3], p. 164).

Comparing equation 1 to the actual data, that is the inter-individual medians of the listening experiment results, deviations up to 106% occur, especially at low frequencies (cf. figure 1). In the remainder of this paper, the arithmetic-mean value and the maximum of the frequency-dependent magnitude of the relative deviation

$$d(f) = \left[\frac{F(f)}{R(f)} - 1\right] \qquad (2)$$

between a function (F) and the corresponding reference-data set (R) will be given as a measure of similarity between function and reference in the form

$$p_{\,F,\,R} = \{100 \cdot \mathrm{avg}\,|d(f)|\,, 100 \cdot \max|d(f)|\}\,\%. \qquad (3)$$

For the comparison of equation 1 to the underlying data of table I, the similarity measure defined by equation 3 results to $p_{\mathrm{Z,\,TI}} = \{21, 106\}\,\%$. This indicates that equation 1 predicts bandwidths deviating up to 106% from the actual data, with an arithmetic average of the deviation's magnitude of 21% (the percentages are rounded to the nearest integer). When comparing two functions, greater similarity that is better agreement with the reference is assumed if $\mathrm{avg}\,|d(f)|$ is smaller by more than 5% for one of the functions, and if at the same time $\max|d(f)|$ is not larger by more than 5%. Thereby, the average agreement is somewhat emphasized in its importance towards good agreement over the maximum value. However, the latter is taken into account, but with reduced importance. As determining the frequency dependence of critical bandwidth is the actual task, it is not clear whether an absolute or a relative similarity measure is suited better for comparing functions and reference. For that reason, an additional visual comparison of functions and data is considered as important as the numerical evaluation according to equation 3.

Table II. Studies the equivalent-rectangular-bandwidth estimates discussed in the present paper were taken from, with the respectively examined density levels (average) and numbers of participants N.

ID	Study	Data	Density levels	N
9 a	Patterson 1976 [18]	Table I (b)	40 dB	4 to 5
9 b	Patterson 1976 [18]	Table A-II (b)	40 dB	3 to 5
10	Houtgast 1977 [36]	Figure 7 (masking)	25, 30, 45 dB	5
11	Weber 1977 [37]	Table III	10, 20, 30, 40, 50 dB	3
12	Shailer & Moore 1983 [38]	Figure 4 (triangles)	40 dB	3
13 a	Fidell et al. 1983 [25]	Table III (1-par. fit)	60 dB	1 to 4
13 b	Fidell et al. 1983 [25]	Table III (2-par. fit)	60 dB	1 to 4
14	Dubno & Dirks 1989 [39]	Table II	40 dB	9
15	Moore et al. 1990 [40]	Section IV	60 dB	6
16	Shailer 1990 [41]	Table II	20, 35, 50 dB	3
17	Jurado & Moore 2010 [42]	Table I, II	50, 62 dB	4 to 11

Traunmüller [14] derived a simplified set of analytic expressions for applying the critical-band concept in the frequency range $0.27 < f/\mathrm{kHz} < 5.8$ to speech technology. Going beyond the frequency range targeted by Traunmüller, his critical-bandwidth function is shown for the full audible frequency range by the dotted black contour in figure 1, as a function valid for the whole audio spectrum is targeted here. While Traunmüller's formula is closer to the actual data at low frequencies than Zwicker and Terhardt's, considerable deviations occur at the upper end of the audible frequency range (cf. figure 1, $p_{\mathrm{T,\,TI}} = \{18, 103\}\,\%$).

Aiming at a formula deviating as little as possible from the data tabulated by Zwicker [12], and at the same time avoiding the selection of negative frequencies described above, Völk ([15], subscript V) proposed an extension to Zwicker and Terhardt's critical-bandwidth function. The resulting formula

$$\Delta f_{\mathrm{G_V}}(f) = \Delta f_{\mathrm{G_Z}}(f)\left(1 - \frac{1}{\left(38.73\,\frac{f}{\mathrm{kHz}}\right)^2 + 1}\right), \quad (4)$$
$$\text{with } 0 \leqslant f \leqslant 20\,\mathrm{kHz}$$

fulfills $\Delta f_{\mathrm{G}}(f) \leqslant 2f\ \forall f$, while fitting the sample values $\Delta f_{\mathrm{G}}[n]$ of Zwicker [12] with an accuracy of $\pm 10\%$ for $n = 1, \ldots, 24$ (cf. dashed black contour in figure 1). As Völk's function is intended to increase the technical applicability of Zwicker and Terhardt's formula in the low-frequency range while otherwise modifying the predicted bandwidths as little as possible, the deviation from the actual data decreases only slightly ($p_{\mathrm{V,\,TI}} = \{20, 93\}\,\%$). The shape of this formula at frequencies below 50 Hz is motivated only by signal-processing constraints, not by psychoacoustic results. Consequently, equation 4 must be primarily interpreted as a proposal aiming at unifying low-frequency implementations of the critical-band concept according to Zwicker and Terhardt's formula (equation 1), not as a better fit to the actual psychoacoustic data.

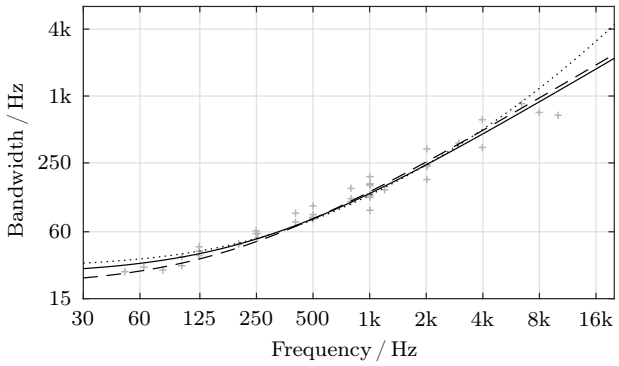

Figure 2. Inter-individual medians of the studies given in table II (gray crosses). Black contours: Equivalent-rectangular bandwidth $\Delta f_{\mathrm{E}}(f)$ according to Moore and Glasberg ([16] dotted, [17] dashed, and [34, 35] solid; the latter is also given by equation 5 of the present paper).

3. Equivalent-rectangular bandwidth

Moore and Glasberg updated their originally proposed formula [16] for the dependence of equivalent-rectangular bandwidth $\Delta f_{\mathrm{E}}(f)$ on frequency twice [17, 34]. Figure 2 shows all three versions (in chronological order: black dotted [16], dashed [17], and solid [34]).

The most recent function,

$$\frac{\Delta f_{\mathrm{E}}(f)}{\mathrm{Hz}} = 24.7\left(4.37\,\frac{f}{\mathrm{kHz}} + 1\right), \quad (5)$$

was reprinted by Moore 2004 ([35], p. 73). The studies quoted by [16, 17, 34] as source or validation data for the formulae are summarized, combined with more recent work, in table II.

The equivalent-rectangular-bandwidth estimates of the studies listed in table II are depicted per study as gray symbols in figure 2. The crosses represent inter-individual medians at different center frequencies. Comparing the

AUTHOR-ACCEPTED MANUSCRIPT OF THE ARTICLE
PUBLISHED IN ACTA ACUSTICA UNITED WITH ACUSTICA, VOL. 101 (2015) 1157 – 1167

most recent formula (equation 5, solid contour in figure 2) to the inter-individual medians of the listening experiment results (gray crosses), deviations up to 62% occur ($p_{\mathrm{E,\,TII}} = \{14, 62\}\,\%$).

4. Critical-band rate

The critical-band rate scale is a frequency scale warped in an auditory-adapted manner, based on the critical bandwidths. It was developed based on the finding that the human hearing system analyzes broadband sounds in spectral sections corresponding to the critical bands ([3], p. 158). Consequently, the frequency dependence of the critical-band rate, assigned the unit Bark, is helpful for modeling characteristics of the human hearing system. According to Zwicker and Terhardt ([13], subscript Z), *critical bandwidth is approximately proportional to the reciprocal of the first derivative of critical-band rate as a function of frequency* (cf. also [3], p. 159). Implementing this dependency, the critical-band-rate function $z_{\mathrm{Z}}(f)$ was defined as an interpolation of the integer valued, tabulated sample points $z[m] = m\,\mathrm{Bark}$, with $m = 0, \ldots, 24$, corresponding to the also tabulated frequencies $f_{\mathrm{l}}[m]$ (black squares in figure 3; [3], p. 160). The frequencies $f_{\mathrm{l}}[m]$ were taken from the limits of the tabulated 24 critical bands, seamlessly arranged on the frequency scale beginning at $f_{\mathrm{l}}[0] = 0$, so that the upper limiting frequency of each band with center frequency $f_{\mathrm{c}}[\kappa]$ equals the lower limiting frequency of the next-higher band according to

$$f_{\mathrm{l}}[\kappa+1] = f_{\mathrm{l}}[\kappa] + \Delta f_{\mathrm{G_Z}}\left(f_{\mathrm{c}}[\kappa]\right),\ \kappa = 0, \ldots, 23. \quad (6)$$

$\Delta f_{\mathrm{G_Z}}(f_{\mathrm{c}}[\kappa])$ grows with κ that is with frequency (black squares in figure 1; cf. [3], p. 160).

Zwicker and Terhardt ([13], subscript Z) proposed, based on the sample values given in [1, 12], the analytic expression

$$\frac{z_{\mathrm{Z}}(f)}{\mathrm{Bark}} = 13 \arctan\frac{0.76 f}{\mathrm{kHz}} + 3.5 \arctan\left(\frac{f}{7.5\,\mathrm{kHz}}\right)^2 \quad (7)$$

for the frequency dependence of critical-band rate (solid black contour in figure 3, cf. [3], p. 164). While fitting the tabulated sample points with an accuracy of $\pm 0.2\,\mathrm{Bark}$, the applicability of equation 7 is limited, for being not invertible in closed form. Furthermore, $z_{\mathrm{Z}}(f)$ tends to underestimate critical-band rate at $f > 16\,\mathrm{kHz}$, as for example, $z_{\mathrm{Z}}(20\,\mathrm{kHz}) \approx 24.58\,\mathrm{Bark}$, while the critical bandwidth of the highest critical band tabulated is $\Delta f_{\mathrm{G_Z}}(f_{\mathrm{l}}[23]) = 3.5\,\mathrm{kHz}$. If the critical bandwidth is assumed to continue growing disproportionately with frequency for $f > 15.5\,\mathrm{kHz}$, a bandwidth in the range of $\Delta f_{\mathrm{G_Z}}(f_{\mathrm{l}}[24]) = 4.5\,\mathrm{kHz}$ appears reasonable. Hence, according to equation 6,

$$\begin{aligned} f_{\mathrm{l}}[25] &= f_{\mathrm{l}}[24] + \Delta f_{\mathrm{G_Z}}\left(f_{\mathrm{l}}[24]\right) \\ &= (15.5 + 4.5)\,\mathrm{kHz} = 20\,\mathrm{kHz} \end{aligned} \quad (8)$$

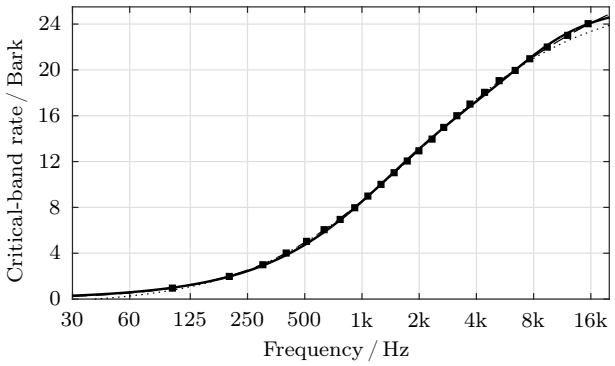

Figure 3. Critical-band rate $z(f)$ as a function of frequency f according to Zwicker and Terhardt ([13], solid; equation 7 of the present paper), Traunmüller ([14], dotted), and Völk ([15], dashed; equation 9 of the present paper). Black squares: tabulated values according to Zwicker 1961 [12].

and the hypothetic critical-band-rate sample $z[25] = 25\,\mathrm{Bark}$ would be reached at $f_{\mathrm{l}}[25] = 20\,\mathrm{kHz}$. Consequently, $z_{\mathrm{Z}}(20\,\mathrm{kHz}) \approx 24.58\,\mathrm{Bark}$ according to equation 7 underestimates the critical-band rate at $f = 20\,\mathrm{kHz}$.

Traunmüller's formulae [14] contain an invertible critical-band-rate function, defined for $200\,\mathrm{Hz} < f < 6.7\,\mathrm{kHz}$, where it fits the original samples with an accuracy of $\pm 0.05\,\mathrm{Bark}$. At frequencies outside this range, it deviates by up to $0.73\,\mathrm{Bark}$ from the tabulated values (dotted contour in figure 3).

Völk [15] proposed the invertible relation of critical-band rate to frequency

$$\frac{z_{\mathrm{V}}(f)}{\mathrm{Bark}} = 32.12\left\{1 - \left[1 + \left(\frac{f/\mathrm{Hz}}{873.47}\right)^{1.18}\right]^{-0.4}\right\}, \quad (9)$$
$$\text{with } 0 \leqslant f \leqslant 20\,\mathrm{kHz},$$

which fits the tabulated values of Zwicker [12] with an accuracy of $\pm 0.08\,\mathrm{Bark}$ (dashed contour in figure 3). Furthermore, equation 9 was fitted to the originally tabulated data extended by the pair $f_{\mathrm{l}}[25] = 20\,\mathrm{kHz}$ and $z[25] = 25\,\mathrm{Bark}$, so that $z_{\mathrm{V}}(20\,\mathrm{kHz}) \approx 24.86\,\mathrm{Bark}$. The inverse of equation 9,

$$\frac{f_{\mathrm{V}}(z)}{\mathrm{Hz}} = 873.47\left[\left(\frac{32.12}{32.12 - \frac{z}{\mathrm{Bark}}}\right)^{2.5} - 1\right]^{\frac{1}{1.18}}, \quad (10)$$
$$\text{with } 0 \leqslant z \leqslant 24.86\,\mathrm{Bark},$$

allows for computing frequencies corresponding to a given critical-band-rate distribution (e. g. equally spaced). The formula of [15] was constructed with the aim of being invertible while representing the tabulated data of [12], not the actual critical-bandwidth data. Therefore, this formula may be considered a more useful implementation of Zwicker and Terhardt's [13] function, not a better fit to the results of listening experiments.

5. Equivalent-rectangular-band rate

Along with the equivalent-rectangular bandwidth, Moore and Glasberg [16, 17, 34] proposed the equivalent-rectangular-band rate (unit E), which may be considered a counterpart to the critical-band rate. The functions are depicted in chronologically ascending order by the dotted [16], dashed [17], and solid [34] contours in figure 4. The invertible most recent [34] version

$$\frac{z_{\mathrm{E}}\,(f)}{\mathrm{E}} = 21.4\,\log_{10}\left(4.37\frac{f}{\mathrm{kHz}}+1\right) \tag{11}$$

(solid black contour in figure 4) was reprinted by Moore (2004 [35], p. 74).

6. Cochlear frequency-position function

Greenwood [31] developed a cochlear frequency-position function, shown to fit physiological data of different species well [43]. In its form given by equation 2 of [31], the function relates the distance x from the apex on the cochlear partition to frequency by

$$f(x) = A(10^{ax/\mathrm{mm}}-1)\,\mathrm{Hz}. \tag{12}$$

The inverse of equation 12 is the corresponding position-frequency function

$$x(f) = \frac{1\,\mathrm{mm}}{a}\log_{10}\left(\frac{f}{A\,\mathrm{Hz}}+1\right). \tag{13}$$

As Greenwood [31, 43] assumed that the critical bands correspond to equally-long sections of the cochlea, $x(f)$ may also be considered Greenwood's (subscript G) critical-band rate $z_{\mathrm{G}}\,(f)$. For humans, Greenwood [43] suggested the parameters $A = 165.4$ and $a = 0.06$. The corresponding bandwidth-position function

$$\Delta f_{\mathrm{G_G}}\,(x) = \frac{\mathrm{d}f}{\mathrm{d}x} = a\ln 10\,A\,10^{ax/\mathrm{mm}}\,\mathrm{Hz} \tag{14}$$

is, according to [31] (equation 2), the first derivative of the frequency-position function $f(x)$. Inserting equation 13 in 14 yields Greenwood's critical bandwidth

$$\Delta f_{\mathrm{G_G}}\,(f) = a\ln 10\,(f/\mathrm{Hz}+A)\ \mathrm{Hz} \tag{15}$$

as a function of frequency. This function has been validated and is physiologically reasonable with different parameters a and A for different species and experiments [31, 43]. Consequently, equation 15 appears to be a reasonable basis function for fitting the psychoacoustic critical-bandwidth and equivalent-rectangular-bandwidth estimates discussed above. Using equation 13, the same parameter set also defines an invertible critical-band-rate function.

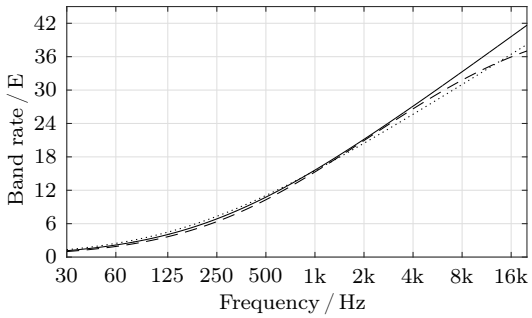

Figure 4. Equivalent-rectangular-band rate $z_{\mathrm{E}}\,(f)$ according to Moore and Glasberg ([16] dotted, [17] dashed, and [34, 35] solid; the latter is also given by equation 11 of the present paper).

7. Fitting procedure and results

From each study of tables I and II, the inter-individual medians of the results per frequency and per experiment were used as the fitting targets. The actual fitting procedure was a nonlinear least-squares regression of equation 15 with the respective target, implemented using the MATLAB® R2015a curve-fitting toolbox (version 3.5.1). Along with the procedure's default settings, two custom settings were used: first, the allowed parameter range was limited to positive values, as only positive bandwidths not decreasing with increasing frequency are in line with Greenwood's framework [31]. Second, the regression was not only carried out without weighting (default setting), but also with weighting the target-bandwidths before the fitting with the inverse of the corresponding center frequency. The weighting was intended to give each data point frequency-independently the same impact on the fitting result, in order to avoid overemphasizing the high-frequency range with larger bandwidths.

Using a least-squares regression as the fitting procedure and the relative measure of similarity defined by equation 3 for comparing functions can cause situations where the similarity-measure rankings differ from the regression results. For that reason, combining the regression results, which are based on absolute differences, with the relative similarity measure and a visual inspection is considered a reliable way of comparing different functions.

7.1. Fitting results: Individual experiments

An individual fitting was carried out for all experiments of tables I and II providing results for more than three different center frequencies and with the lowest center frequency below 400 Hz. All data sets fulfilling these requirements span at least three octaves within the audible frequency range. Studies with fewer center frequencies were included in the target for the fitting to the pooled data discussed below, but do not provide valid fitting targets for individual broadband functions. The fitting results, that is the parameters a and A of equation 15, for the accordingly relevant experiments of tables I and II are given in tables III and IV, respectively.

Table III. Results of fitting equation 15 to the median results of each experiment of the studies listed in table I containing more than four center frequencies. No brackets: data weighted by inverse center frequency; brackets: no weighting.

ID	a	A
1	0.083 (0.094)	211.2 (0.0)
2	0.079 (0.080)	273.4 (210.6)
3	0.070 (0.074)	334.3 (155.2)
6	0.059 (0.062)	254.9 (152.8)
7 a	0.041 (0.037)	661.0 (789.7)
7 b	0.046 (0.047)	359.1 (341.3)
8 a	0.054 (0.056)	488.4 (429.9)
8 b	0.056 (0.062)	331.4 (69.0)
Median	0.057 (0.062)	332.9 (182.9)
Mean	0.061 (0.064)	364.2 (268.6)

Table IV. Results of fitting equation 15 to the median results of each experiment of the studies listed in table II containing more than four center frequencies. No brackets: data weighted by inverse center frequency; brackets: no weighting.

ID	a	A
10	0.066 (0.064)	169.4 (211.6)
12	0.055 (0.057)	147.4 (64.6)
13 a	0.039 (0.038)	379.3 (403.8)
13 b	0.046 (0.046)	248.6 (250.2)
14	0.043 (0.045)	363.6 (300.0)
15	0.070 (0.070)	115.6 (114.7)
17	0.060 (0.059)	136.6 (138.4)
Median	0.057 (0.058)	158.4 (175.0)
Mean	0.056 (0.056)	199.5 (197.2)

The identifiers (ID) of the studies correspond between the tables and across the paper. An ID occurring more than once indicates that the respective study contains data of multiple experiments, each fitted individually and indicated by additional lower-case letters. Every resulting parameter is given twice, without brackets for the fitting procedure with inverse-frequency weighting, and within brackets for fitting with no weighting. At the bottom, the tables show the averages of the parameters (medians and arithmetic mean values).

Figures 5 and 6 contain the results of the studies from tables I and II, respectively, as gray symbols in the background. Additionally, the fitting results of the procedure with inverse-frequency weighting (indicated by no brackets in tables III and IV) are shown as solid black contours. The panels in parts a) represent the individual fits and data, the solid black contour in panels b) indicates the function constructed using equation 15 and the respectively corresponding medians of the parameters a and A. Furthermore, panels b) show all data of the respective table (I or II, gray crosses). For comparison purposes, figures 5 and 6

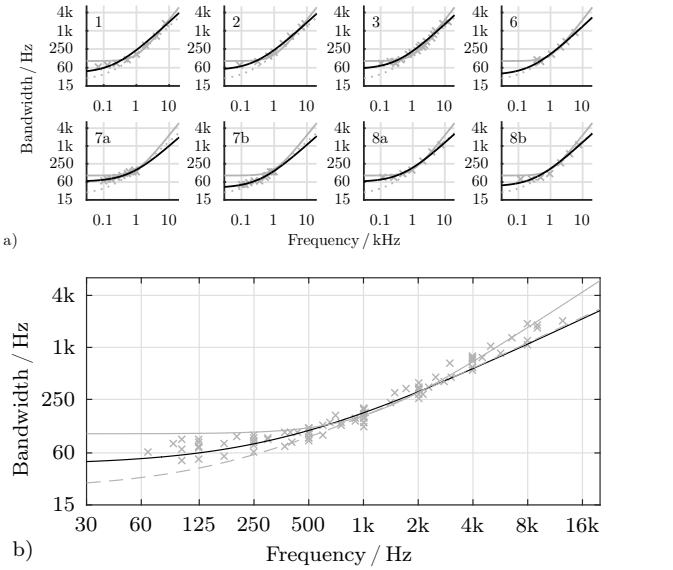

Figure 5. a) Individual fitting results (black contours) of equation 15 to the results of the studies in table I. Each panel represents one experiment (insert: IDs), gray crosses indicate the respective results. b) Fitting result when using the parameter median (solid black, cf. table III), and all data of table I (gray crosses). a) & b) Gray contours: Critical bandwidths according to Zwicker and Terhardt ([13], solid) and Greenwood ([43], dashed).

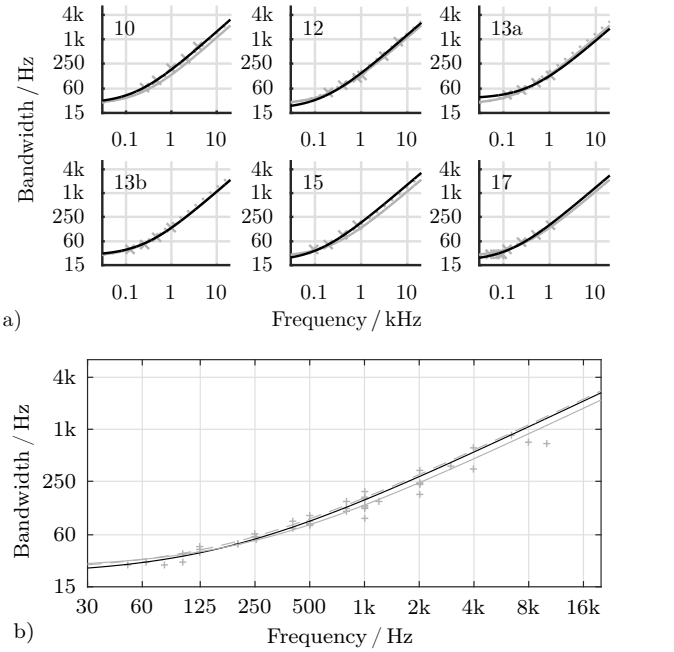

Figure 6. a) Individual fitting results (black contours) of equation 15 to the results of the studies in table II. Each panel represents one experiment (insert: IDs, gray crosses: results). b) Fitting result when using the parameter median (solid black, cf. table IV), and all data of table II (gray crosses). a) & b) Gray contours: Equivalent-rectangular bandwidth according to Glasberg and Moore ([34], solid) and critical bandwidth according to Greenwood ([43], dashed).

contain also the critical bandwidth respectively equivalent-rectangular bandwidth functions. Both figures show the

critical-bandwidth function according to Greenwood ([43], equation 15 with $a = 0.06$ and $A = 165.4$, dashed gray contour). Additionally, the solid gray contours represent critical-bandwidth according to Zwicker and Terhardt [13] in figure 5 and equivalent-rectangular bandwidth according to Glasberg and Moore [34] in figure 6.

7.2. Fitting results: Pooled data

The fitting process was also carried out with the pooled results of all studies as the fitting target, per table (I and II) and overall. Table V shows the parameters resulting from fitting equation 15 to the pooled data of tables I and II, separately (rows I and II), and to the combined data of both tables (row I&II). Additionally, the medians over the parameters are reprinted from tables III and IV, for comparison purposes. For the same reason, the parameters suggested or proposed by earlier studies are included (parameters a and A for [34] derived from equation 5).

Figure 7 shows the results of all studies from tables I and II as gray symbols in the background. In addition, the critical bandwidths according to Zwicker and Terhardt ([13], solid gray) and Greenwood ([43], dashed gray), as well as the equivalent-rectangular bandwidth according to Glasberg and Moore ([34], dotted gray) were included for comparison purposes. The actual fitting results for the inverse-frequency-weighted procedure (no brackets in table V) are shown in black. The solid and dotted black contours represent the formulae fitted to the pooled data of tables I and II, respectively. The dashed black contour indicates the function fitted to the pooled data of both tables.

Table V. Results of fitting equation 15 to the pooled median results of all experiments of tables I and II, separately (I, II) and overall (I&II). Also shown are the corresponding medians of the parameters from the individual fits (tables III and IV), and earlier proposals. No brackets: data weighted by inverse center frequency; brackets: no weighting.

ID	a	A
I	0.069 (0.074)	264.0 (98.7)
Median Tab. III	0.057 (0.062)	332.9 (182.9)
II	0.045 (0.038)	261.3 (584.3)
Median Tab. IV	0.057 (0.058)	158.4 (175.0)
1&2	0.063 (0.065)	231.7 (158.7)
Median Tab. III & IV	0.057 (0.061)	264.2 (182.9)
Greenwood [43]	0.060	165.4
Glasberg & Moore [34]	0.047	228.8

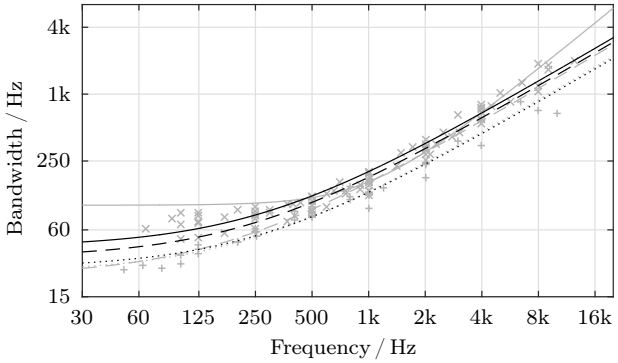

Figure 7. Results of the studies in tables I (×) and II (+). Gray contours: critical bandwidths according to Zwicker and Terhardt ([13], solid) and Greenwood ([43], dashed), equivalent-rectangular bandwidth according to Glasberg and Moore ([34], dotted). Black contours: fits of equation 15 to the data per table (cf. rows of table V: I solid, II dotted) and all data (row I&II, dashed).

8. Discussion

Tables III, IV, and V indicate mostly moderate differences between the data within and without brackets. The results of study 1 (ID 1) only allowed for a non-linear fit (that is $A \neq 0$) with inverse-frequency weighting (represented by the unbracketed data). Therefore, giving the data frequency independently comparable influence on the fitting procedure by inverse-frequency weighting appears to be more in line with Greenwood's assumptions [31, 43] than the unweighted fitting. Additionally, comparable dependencies and conclusions arise for both data sets. For these reasons, the results of the weighted fitting procedure are discussed in the following.

8.1. Critical bandwidth

Figure 5 reveals that the frequency-bandwidth function proposed by Zwicker and Terhardt ([13], equation 1, solid gray contours in figure 5) tends, at center frequencies below 500 Hz and above 4 kHz, to overestimate the critical-bandwidth results of the studies listed in table I (gray symbols in figure 5). These tendencies are somewhat reflected in the maximum of the relative deviation $p_{\mathrm{Z,\,TI}} = \{21, 106\}\,\%$ between formula and data, and in the differences between equation 1 (solid gray contours in figure 5) and the functions fitted to the individual experiments (black contours in figure 5 a). The fitted functions proceed steeper than equation 1 below some 450 Hz and shallower above about 4 kHz, that is to say with less curvature. Summarizing this paragraph, the frequency-bandwidth function given by equation 1 cannot be considered an exact or average representation of the bandwidth estimates of the studies listed in table I.

Comparing the data (gray symbols in figure 5) and individually-fitted functions (black contours in figure 5 a) to Greenwood's frequency-bandwidth formula (equation 15) with the parameters for humans of [43] ($a = 0.06$ and $A = 165.4$, dashed gray contours in figure 5) indicates a fairly well agreement in the frequency range above about 1 kHz. At lower frequencies, Greenwood's function underestimates the data of table I by more

AUTHOR-ACCEPTED MANUSCRIPT OF THE ARTICLE
PUBLISHED IN ACTA ACUSTICA UNITED WITH ACUSTICA, VOL. 101 (2015) 1157 – 1167

than 50%, reflected also by $p_{\mathrm{G,\,TI}} = \{19, 58\}\,\%$. Taking into account that the bandwidths predicted by equation 15 at the upper limit of the audible frequency range are dominated by the parameter a, the results of tables III and V with average values between $a = 0.057$ and $a = 0.074$ closely confirm Greenwood's $a = 0.06$ [43]. However, the parameter A, considerably influencing the function's low-frequency shape, is predicted in a wide range between somewhat smaller and up to more than 100% larger than Greenwood's [43] recommendation $A = 165.4$ (average values from $A = 98$ to $A = 365$). As a consequence, also equation 15 with the parameters of Greenwood [43] is not considered a well-suited representation of the listening experiment results of the studies in table I, if the full audible frequency range is targeted.

Equation 15 with the median parameters resulting from the fitting procedures as given by table III (solid black contour in figure 5) fits the data of table I with $p_{\mathrm{TIII_{Med},\,TI}} = \{15, 42\}\,\%$ (cf. figure 5). A comparable agreement results when using the parameters fitted to the pooled data of table I (table V, row I, $p_{\mathrm{TV_1,\,TI}} = \{17, 63\}\,\%$).

8.2. Equivalent-rectangular bandwidth

Globally, the equivalent-rectangular-bandwidth function of Glasberg and Moore (equation 5, solid gray contour in figure 6) fits the data of the studies listed in table II (gray symbols) rather well, with $p_{\mathrm{E,\,TII}} = \{14, 62\}\,\%$. A tendency is visible for a somewhat flatter high-frequency shape of equation 5 (solid gray contour), compared to the fitting results (solid black), and also compared to Greenwood's function (equation 15), with the parameters of [43] for humans (dashed gray contour in figure 6).

The latter function represents the data of table II with $p_{\mathrm{G,\,TII}} = \{20, 107\}\,\%$, the function with the fitted parameters with $p_{\mathrm{TIV_{Med},\,TII}} = \{16, 96\}\,\%$. Notably, the medians of the parameters resulting from the fitting procedure (table IV, $a = 0.057$, $A = 158.4$) closely resemble Greenwood's proposal ([43], $a = 0.06$, $A = 165.4$). Equation 15 with the parameters fitted to the pooled data of table II (table V, row II) agrees to a similar extent with the data ($p_{\mathrm{TV_2,\,TII}} = \{14, 56\}\,\%$).

8.3. Combined results

Table V indicates that fitting equation 15 to the pooled data (rows I, II, I&II) and individual fitting (Medians) resulted in comparable parameters, for the single as well as for the combined data sets. For that reason, and because the pooled data provide a broader spectral coverage than the individual data, the fitting results for the pooled data are shown in figure 7 and discussed in the following.

Looking at the overall bandwidth-data set (gray symbols in figure 7), again the low-frequency and high-frequency overestimation of Zwicker and Terhardt's function (equation 1, solid gray contour) becomes visible. This is reflected in $p_{\mathrm{Z,\,TI\&II}} = \{41, 227\}\,\%$. Equation 15 fitted to the pooled data of table I (solid black contour) represents the whole data set better, with $p_{\mathrm{TV_1,\,TI\&II}} = \{30, 140\}\,\%$.

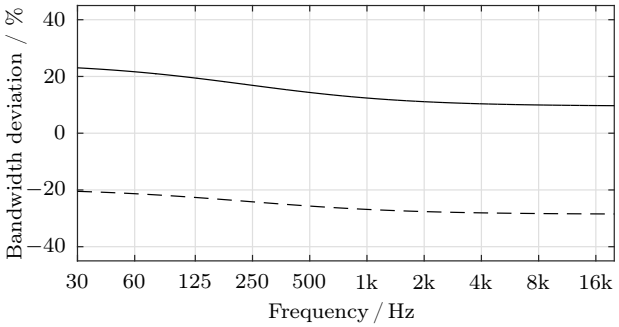

Figure 8. Relative deviation of equation 15 fitted to the data of table I (solid) and table II (dashed) from equation 15 fitted to the pooled data.

Glasberg and Moore's bandwidth function (equation 5, dotted gray contour in figure 7) and equation 15 fitted to the pooled data of table II (dotted black contour) represent the overall data set with comparable accuracies ($p_{\mathrm{E,\,TI\&II}} = \{24, 57\}\,\%$ vs. $p_{\mathrm{TV_2,\,TI\&II}} = \{24, 62\}\,\%$). Figure 7 again reveals the tendency for both functions to underestimate the high-frequency section of the data.

Greenwood's bandwidth function (equation 15) with the parameters of [43] for humans (dashed gray contour in figure 7) is comparable to the function fitted to the data of table II at low center frequencies (dotted black), and to the function fitted to the data of table I in the high-frequency range (solid black). Compared to the pooled data, a deviation of $p_{\mathrm{G,\,TI\&II}} = \{19, 107\}\,\%$ occurs.

Equation 15 fitted to the overall-pooled data results in $p_{\mathrm{TV_{1\&2},\,TI\&II}} = \{22, 118\}\,\%$, indicated by the dashed black contour in figure 7. Compared to Greenwood's parameters (dashed gray contour), this function visually appears to represent the overall data set (gray crosses) at low frequencies below some 250 Hz better, as suggested by the regression, even tough $p_{\mathrm{G,\,TI\&II}} = \{19, 107\}\,\%$ shows an opposing tendency.

Comparing the functions fitted to the data of table I, the data of table II, and the pooled data (black contours in figure 7) reveals similar shapes, but different vertical positions that is different bandwidths. However, the relative vertical displacement between the contours appears to be approximately frequency independent. In order to quantify the similarity between these three functions, figure 8 shows the relative deviations of the functions fitted to the data of tables I (solid) and II (dashed) from the function fitted to the pooled data.

Both deviations shown in figure 8 depend to some extent on frequency. The function fitted to the data of table I (solid contour) proceeds $(17.2 \pm 7.5)\%$ above the function fitted to the pooled data, predicting some 1.09 to 1.25 times larger bandwidths. Fitting equation 15 to the data of table II results in about 0.71 to 0.81 times smaller bandwidths than fitting to the overall-pooled data, which means a deviation of $(-24 \pm 4.5)\%$ between the contours.

For applications where the frequency dependencies listed in the previous paragraph are tolerable, it is possible to use

the critical-bandwidth function fitted to the overall-pooled data and adjust it with frequency independent factors to the respectively desired data set (1.17 for the data of table I and 0.76 for that of table II).

9. Summary and proposed functions

The analysis and discussion of earlier critical-bandwidth estimates conducted in this paper supports the structure of the analytical critical-bandwidth-frequency function proposed by Greenwood [31, 43]. The function as given by equation 15 was fitted to two data sets, namely the data used earlier to construct and validate Zwicker and Terhardt's [13] critical-bandwidth function (equation 1) and the data used by Glasberg and Moore [34] to derive and confirm their equivalent-rectangular-bandwidth function (equation 5). With the parameters $a = 0.069$ and $A = 264$ derived from the pooled data of table I (related to Zwicker and Terhardt's formula) and $a = 0.045$ and $A = 261$ derived from the pooled data of table II (related to Glasberg and Moore's latest function), equation 15 deviates less than 50% from 50% of the respective data. Comparable deviations were also achieved by multiplying frequency independent constants c with the function resulting from fitting equation 15 to the pooled data used by Zwicker and Terhardt as well as Glasberg and Moore ([13, 34], parameters $a = 0.063$, $A = 232$). Adapting this function with different constants c to both data sets causes a deviation from the individually fitted functions. For the studies included here, the deviations between the approximated and the individually-fitted functions stay for critical bandwidths below 7.8% (with $c = 1.17$), and for equivalent-rectangular bandwidths below 4.6% ($c = 0.76$). Applications that can tolerate these deviations may therefore use the critical-bandwidth-frequency function

$$\Delta f_{\mathrm{G}}(f) = 0.063 \ln 10 \,(f/\mathrm{Hz} + 232)\ \mathrm{Hz}, \tag{16}$$

multiplied with a constant c, selected either as proposed above ($c = 1.17$ for Zwicker and Terhardt, $c = 0.76$ for Glasberg and Moore) or as required by the application.

Greenwood's position-frequency function (equation 13) provides the band-rate function corresponding to his bandwidth formula. With the parameters derived here, the critical-band rate (and at the same time the distance from the apex on the cochlear partition) is, according to Greenwood's concept, given by

$$x(f) = \frac{1\,\mathrm{mm}}{0.063} \log_{10}\left(\frac{f}{232\,\mathrm{Hz}} + 1\right). \tag{17}$$

The inverse, Greenwood's actual starting point given by equation 12, the frequency-position function

$$f(x) = 232\,(10^{0.063x/\mathrm{mm}} - 1)\,\mathrm{Hz}, \tag{18}$$

is required for calculating a set of frequencies approximately equally spaced on the cochlea, according to Greenwood's concept with the parameters derived here.

Equations 16, 17, and 18 provide a closed set of equations for applying the critical-band and equivalent-rectangular-band concepts to digital signal processing that are better in line with the critical-bandwidth estimates of the studies included here than earlier formulae. Especially low-frequency critical bandwidths, which are overestimated by Zwicker and Terhardt's [13] critical-bandwidth function, are represented more accurately by the updated formulae. Additionally, the average data used to justify both concepts can be represented in good approximation by a single function, multiplied with frequency independent constants. Artifacts and shortcomings as for example the undesired selection of negative frequencies and the non-invertibility of the critical-band rate function are reduced or avoided by the proposed functions and parameters. Free software implementations of the suggested formulae are available at `http://www.windacoustics.com` (section `Downloads`).

Acknowledgments

The author is indebted to Prof. Dr.-Ing. Hugo Fastl, Prof. Dr.-Ing. Werner Hemmert, the associate editor, and two anonymous reviewers for extremely valuable comments on earlier versions of the manuscript. Parts of this work were conducted at AG Technische Akustik, MMK, Technische Universität München, supported by Deutsche Forschungsgemeinschaft (Grant FA 140/4).

References

[1] E. Zwicker, G. Flottorp, S. S. Stevens: Critical band width in loudness summation. J. Acoust. Soc. Am. **29** (1957) 548–557.

[2] H. Fletcher, W. A. Munson: Relation between loudness and masking. J. Acoust. Soc. Am. **9** (1937) 1–10.

[3] H. Fastl, E. Zwicker: Psychoacoustics – Facts and models. 3rd ed. Springer, Berlin, Heidelberg, 2007.

[4] E. Zwicker: Die Grenzen der Hörbarkeit der Amplitudenmodulation und der Frequenzmodulation eines Tones (The audibility limits of pure-tone amplitude modulation and frequency modulation). Acustica **3** (1952) AB 125–133.

[5] E. Zwicker, R. Feldtkeller: Über die Lautstärke von gleichförmigen Geräuschen (On the loudness of uniform sounds). Acustica **5** (1955) 303–316.

[6] G. Gässler: Über die Hörschwelle für Schallereignisse mit verschieden breitem Frequenzspektrum (On the threshold in quiet of sounds with frequency spectra of different width). Acustica **4** (1954) 408–414.

[7] E. Zwicker: Die Verdeckung von Schmalbandgeräuschen durch Sinustöne (Masking of narrow-band sounds by pure tones). Acustica **4** (1954) AB 415–420.

[8] E. Terhardt: Fourier transformation of time signals: Conceptual revision. Acustica **57** (1985) 242–256.

[9] M. Mummert: Sprachcodierung durch Konturierung eines gehörangepaßten Spektrogramms und ihre Anwendung zur Datenreduktion (Speech coding by contouring an ear-adapted spectrogram and its application to data reduction). Dissertation. Technische Universität München, 1997.

[10] F. Völk, T. Riesenweber, H. Fastl: Ein Algorithmus zur Vorhersage des für transparente Auralisierung nutzbaren Dynamikbereichs rauschbehafteter Impulsantworten (An algorithm for the prediction of the dynamic range available for transparent auralization in noisy impulse responses). Fortschritte der Akustik, DAGA 2011, 2011, Dt. Gesell. für Akustik e. V., Berlin, 315–316.

[11] F. Völk: Interrelations of virtual acoustics and hearing research by the example of binaural synthesis. Dissertation. Technische Universität München, 2013.

[12] E. Zwicker: Subdivision of the audible frequency range into critical bands (Frequenzgruppen). J. Acoust. Soc. Am. **33** (1961) 248.

[13] E. Zwicker, E. Terhardt: Analytical expressions for critical-band rate and critical bandwidth as a function of frequency. J. Acoust. Soc. Am. **68** (1980) 1523–1525.

[14] H. Traunmüller: Analytical expressions for the tonotopic sensory scale. J. Acoust. Soc. Am. **88** (1990) 97–100.

[15] F. Völk: Updated analytical expressions for critical bandwidth and critical-band rate. Fortschritte der Akustik, DAGA 2015, 2015, Dt. Gesell. für Akustik e. V., Berlin, 1181–1184.

[16] B. C. J. Moore, B. R. Glasberg: Suggested formulae for calculating auditory-filter bandwidths and excitation patterns. J. Acoust. Soc. Am. **74** (1983) 750–753.

[17] B. C. J. Moore, B. R. Glasberg: Formulae describing frequency selectivity as a function of frequency and level, and their use in calculating excitation patterns. Hearing Research **28** (1987) 209–225.

[18] R. D. Patterson: Auditory filter shapes derived with noise stimuli. J. Acoust. Soc. Am. **59** (1976) 640–654.

[19] F. Völk, M. Straubinger, L. Roalter, H. Fastl: Measurement of head related impulse responses for psychoacoustic research. Int. Conference on Acoustics NAG/DAGA 2009, 2009, Dt. Gesell. für Akustik e. V., Berlin, 164–167.

[20] J. L. Verhey, J. Rennies, S. M. A. Ernst: Influence of envelope distributions on signal detection. Acta Acustica united with Acustica **93** (2007) 115–121.

[21] J. Rennies, J. L. Verhey: Temporal weighting in loudness of broadband and narrowband signals. J. Acoust. Soc. Am. **126** (2009) 951–954.

[22] J. Rennies, J. L. Verhey, H. Fastl: Comparison of loudness models for time-varying sounds. Acta Acustica united with Acustica **96** (2010) 383–396.

[23] P. C. Loizou: Mimicking the human ear – An overview of signal-processing strategies for converting sound into electrical signals in cochlear implants. IEEE Signal Processing Magazine **15** (1998) 101–130.

[24] J. Chalupper, H. Fastl: Dynamic loudness model (DLM) for normal and hearing-impaired listeners. Acta Acustica united with Acustica **88** (2002) 378–386.

[25] S. Fidell, R. Horonjeff, S. Teffeteller, D. M. Green: Effective masking bandwidths at low frequencies. J. Acoust. Soc. Am. **73** (1983) 628–638.

[26] E. Schorer: Zum Einfluss der Kopfhörerentzerrung bei der Messung der Frequenzgruppenbreite des Gehörs (On the influcence of the headphone equalization during the measurement of the hearing system's critical bandwidth). Fortschritte der Akustik, DAGA '86, 1986, DPG, Bad Honnef, 437–440.

[27] A. Sek, B. C. J. Moore: The critical modulation frequency and its relationship to auditory filtering at low frequencies. J. Acoust. Soc. Am. **95** (1994) 2606–2615.

[28] A. J. M. Houtsma: Hawkins and Stevens revisited with insert earphones. J. Acoust. Soc. Am. **115** (2004) 967–970.

[29] A. J. M. Houtsma: A note on pure-tone masking by broadband noise under free-field and insert-phone conditions. J. Acoust. Soc. Am. **117** (2005) 490–491.

[30] F. Völk, C. Landsiedel, H. Fastl: Auditory adapted exponential transfer function smoothing (AAS). IEEE Workshop on Applications of Signal Processing to Audio and Acoustics (WASPAA), 2011, 49–52.

[31] D. D. Greenwood: Critical bandwidth and the frequency coordinates of the basilar membrane. J. Acoust. Soc. Am. **33** (1961) 1344–1356.

[32] H. Bauch: Die Bedeutung der Frequenzgruppe für die Lautheit von Klängen (The impact of the critical band on the loudness of sounds). Acustica **6** (1956) 40–45.

[33] E. Schorer: Critical modulation frequency based on detection of AM versus FM tones. J. Acoust. Soc. Am. **79** (1986) 1054–1057.

[34] B. R. Glasberg, B. C. J. Moore: Derivation of auditory filter shapes from notched-noise data. Hearing Research **47** (1990) 103–138.

[35] B. C. J. Moore: An introduction to the psychology of hearing. 5th ed. Elsevier Academic Press, London, San Diego, 2004.

[36] T. Houtgast: Auditory-filter characteristics derived from direct-masking data and pulsation-threshold data with a rippled-noise masker. J. Acoust. Soc. Am. **62** (1977) 409–415.

[37] D. L. Weber: Growth of masking and the auditory filter. J. Acoust. Soc. Am. **62** (1977) 424–429.

[38] M. J. Shailer, B. C. J. Moore: Gap detection as a function of frequency, bandwidth, and level. J. Acoust. Soc. Am. **74** (1983) 467–473.

[39] J. R. Dubno, D. D. Dirks: Auditory filter characteristics and consonant recognition for hearing-impaired listeners. J. Acoust. Soc. Am. **85** (1989) 1666–1675.

[40] B. C. J. Moore, R. W. Peters, B. R. Glasberg: Auditory filter shapes at low center frequencies. J. Acoust. Soc. Am. **88** (1990) 132–140.

[41] M. J. Shailer, B. C. J. Moore, B. R. Glasberg, N. Watson, S. Harris: Auditory filter shapes at 8 and 10 kHz. J. Acoust. Soc. Am. **88** (1990) 141–148.

[42] C. A. Jurado, B. C. J. Moore: Frequency selectivity for frequencies below 100 Hz: Comparisons with mid-frequencies. J. Acoust. Soc. Am. **128** (2010) 3585–3596.

[43] D. D. Greenwood: A cochlear frequency-position function for several species – 29 years later. J. Acoust. Soc. Am. **87** (1990) 2592–2605.